

Supporting Information

Bright G-Quadruplex Nanostructures Functionalized with Porphyrin Lanterns

Pravin Pathak,^a Wei Yao,^a Katherine Delaney Hook,^d Ryan Vik,^a Fernaldo Richtia Winnerdy,^b Jonathon Quincy Brown,^c Bruce C. Gibb,^a Zachary F Pursell,^d Anh Tuân Phan,^b and Janarthanan Jayawickramarajah^{*a}

^aDepartment of Chemistry, Tulane University, 2015 Percival Stern Hall, New Orleans, Louisiana 70118, United States

^bSchool of Physical and Mathematical Sciences, Nanyang Technological University, Singapore 637371, Singapore

^cDepartment of Biomedical Engineering, Tulane University, New Orleans, LA 70118, United States

^dDepartment of Biochemistry and Molecular Biology, Tulane University, New Orleans, LA 70112, United States

Table of Contents

Synthesis schemes of Porph-DNA 1, Porph-DNA 2, PL-DNA 1, PL-DNA 2, and PL-polyT	Fig. S1
MALDI-TOF spectrum of Porph-DNA 1	Fig. S2
MALDI-TOF spectrum of PL-DNA 1.....	Fig. S3
MALDI-TOF spectrum of Porph-DNA 2.....	Fig. S4
MALDI-TOF spectrum of PL-DNA 2	Fig. S5
Synthesis and characterization of Porph-PEG and PL-PEG	Fig. S6
Absorption and Emission profiles of Porph-PEG and PL-PEG	Fig. S7
HPLC traces of Porphyrin-DNA conjugates	Fig. S8
Full UV-Vis absorption spectra of porphyrin-DNA conjugates.....	Fig. S9
Molar absorptivity determination of Porphyrin-DNA species before annealing.....	Fig. S10
Molar absorptivity determination of Porphyrin-DNA species after annealing.....	Fig. S11
CD spectra of non-self-assembling species.....	Fig. S12
Emission profiles of PL-DNA 1 with adamantyl derivative.....	Fig. S13
Quantum yield determination of Porph-DNA 1 and PL-DNA 1 assemblies	Fig. S14
Quantum yield determination of Porph-DNA 2 and PL-DNA 2 assemblies	Fig. S15
AFM images with height profiles	Fig. S16
¹ H NMR of compound 3	Fig. S17
¹³ C NMR of compound 3.....	Fig. S18
¹ H NMR of compound 4	Fig. S19
¹³ C NMR of compound 4.....	Fig. S20
¹ H NMR of Porphyrin 1.....	Fig. S21
¹³ C NMR of Porphyrin 1	Fig. S22
Models of G-wire and unit G-quadruplex	Fig. S23
Decomplexation experiments of PM β CD-Porphyrin self-inclusion complex.....	Fig. S24
Dynamic Light Scattering Experiments	Fig. S25

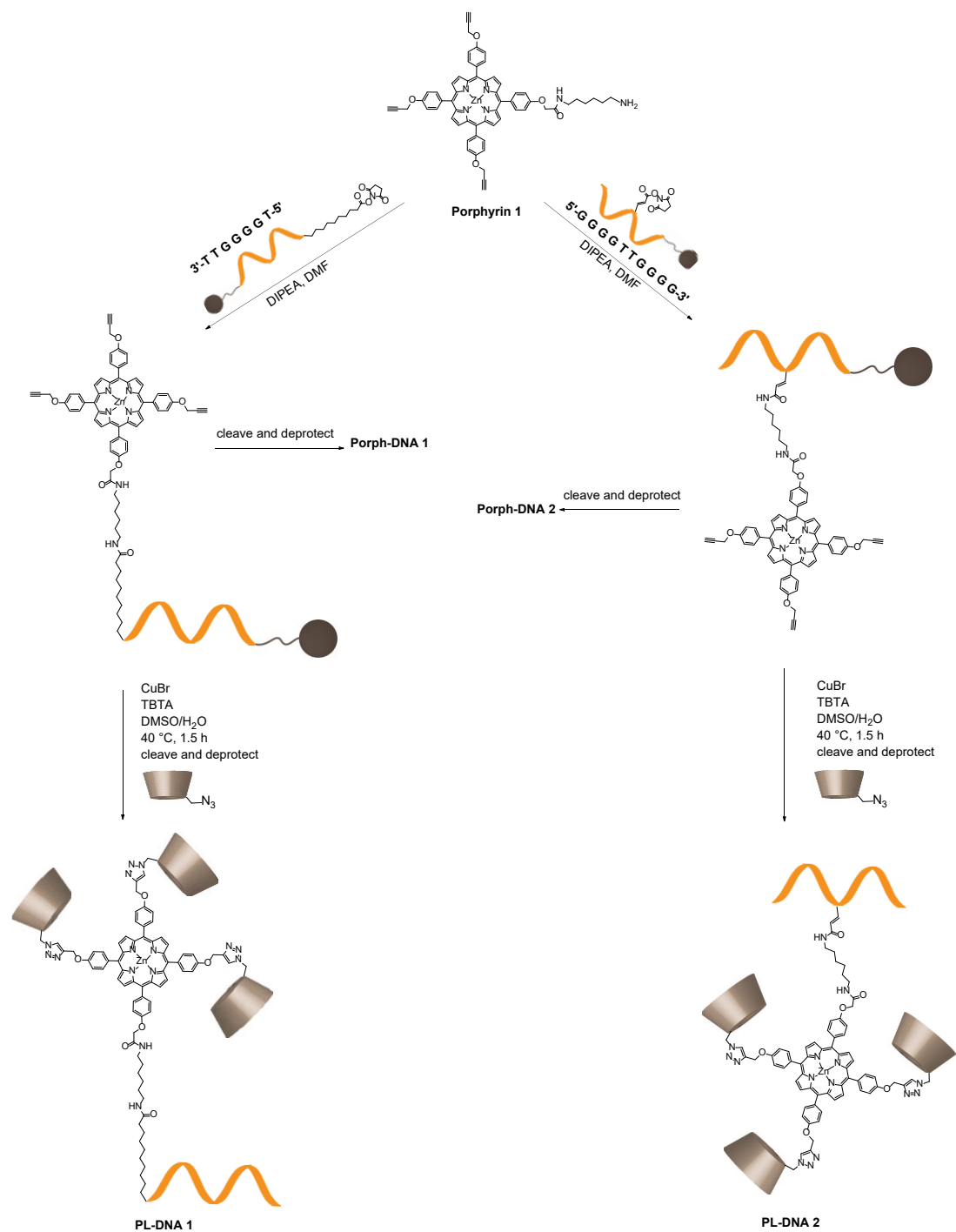


Figure S-1. Synthesis scheme of porphyrin-DNA conjugates illustrating the tethering and masking steps. PL-polyT synthesis (not shown) involved identical steps where the sequence used was 5'-NHS modified T₁₀-3'.

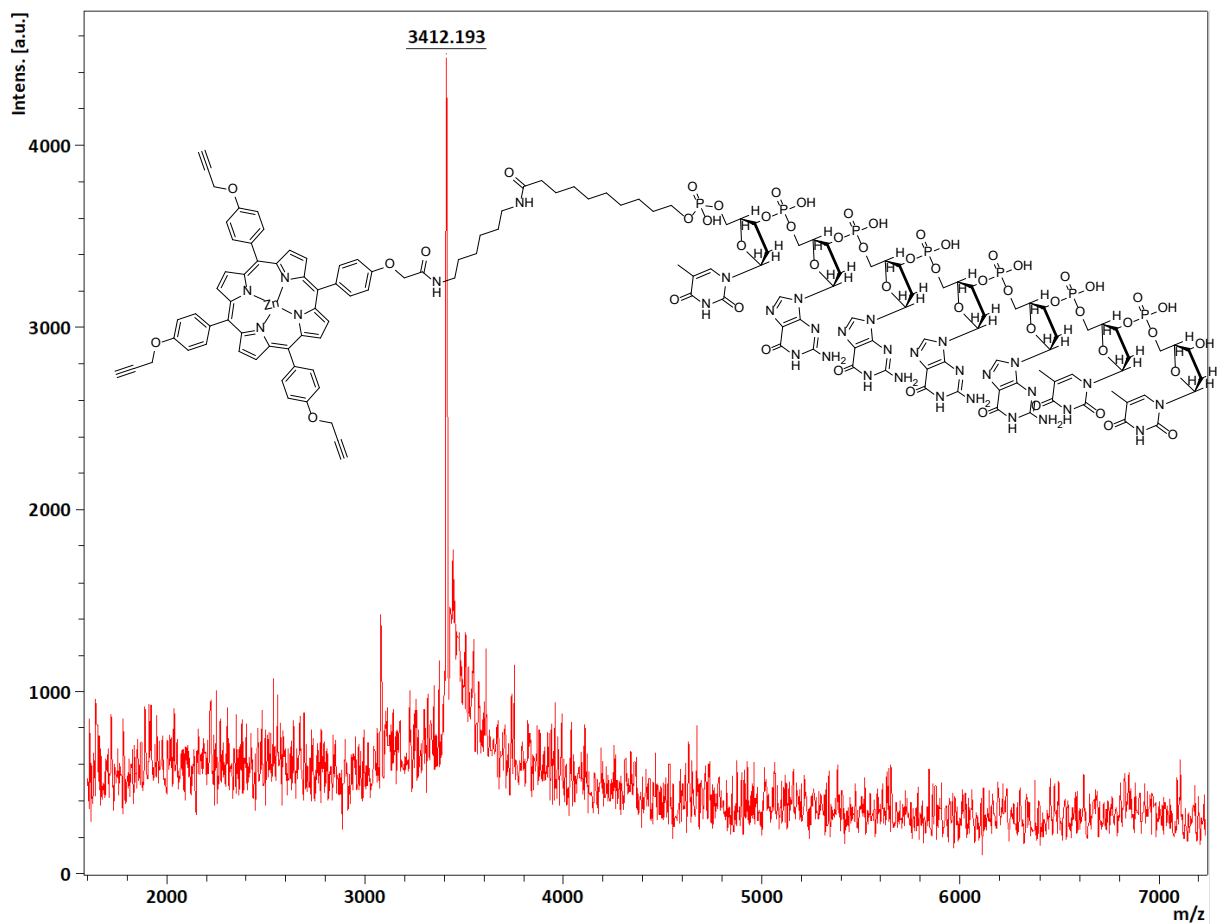


Figure S-2. MALDI-TOF spectrum of Porph-DNA 1, found MW = 3412.19 Da, calculated MW = 3413.17 Da, for $[M+H]^+$.

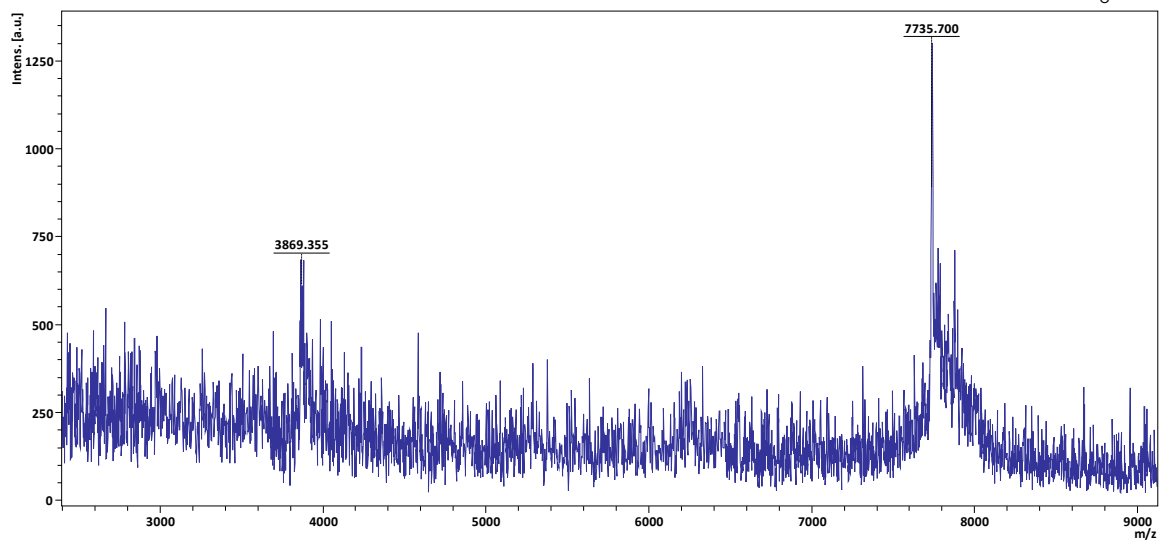
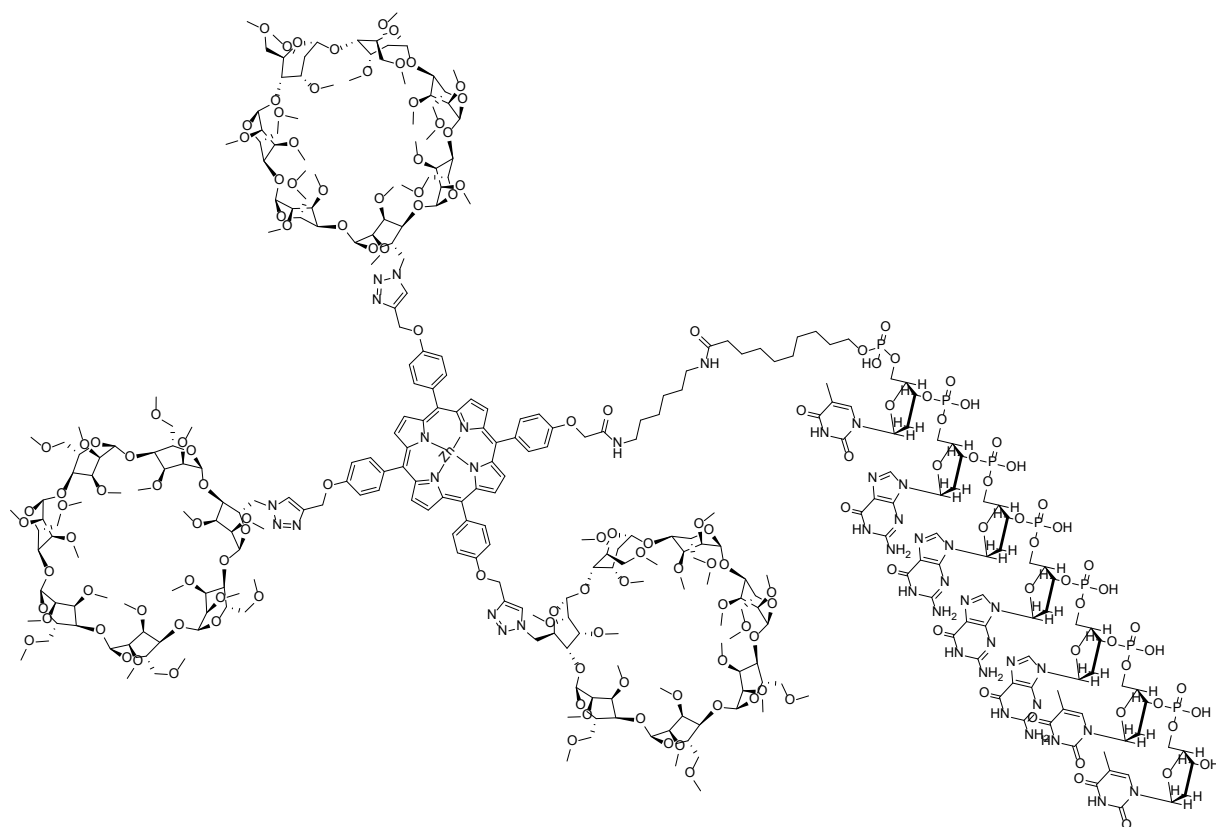


Figure S-3. MALDI-TOF spectrum of PL-DNA 1, found MW = 7735.70 Da, calculated MW = 7734.79 Da, for $[M+H]^+$. Peak at 3869.36 represents $[M+2H]^{++}$.

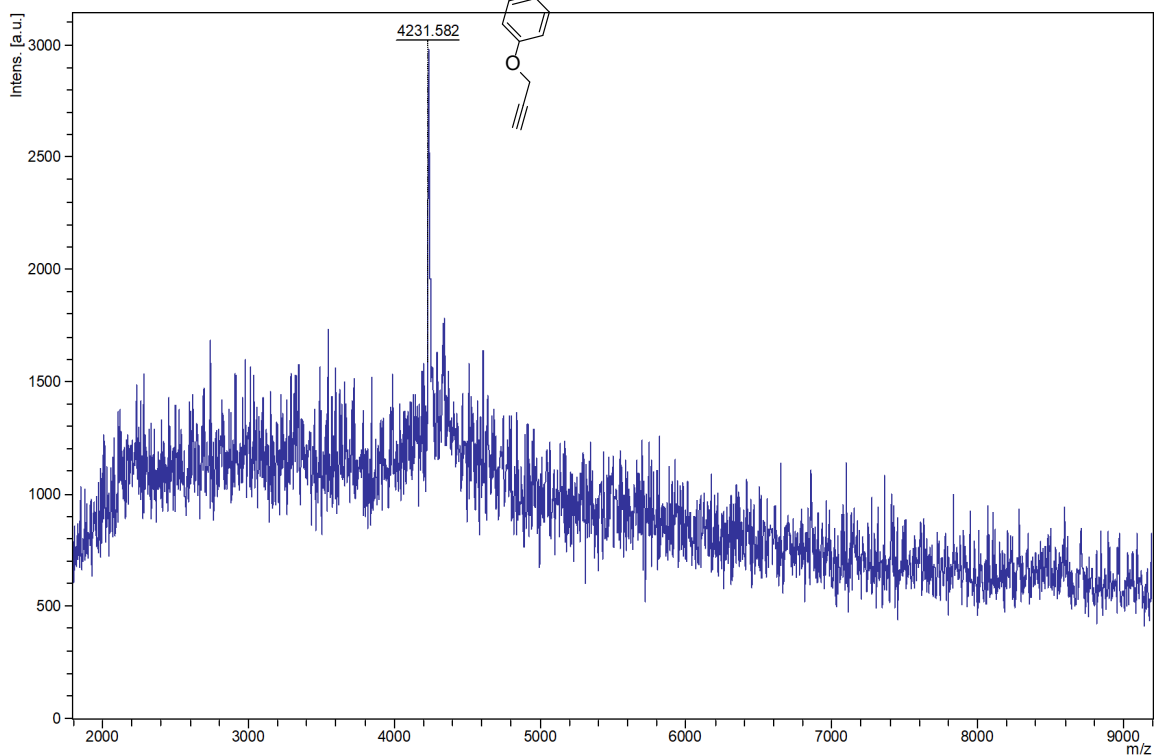
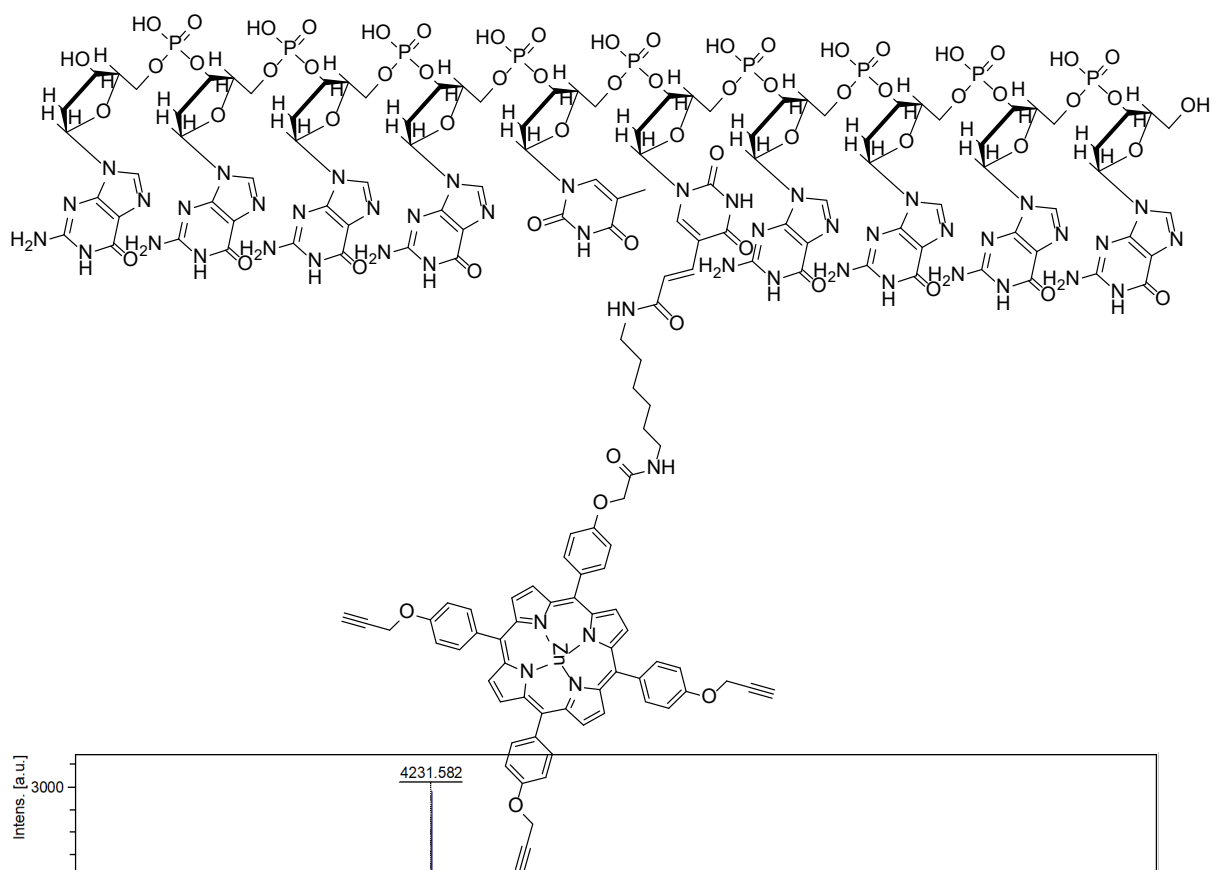


Figure S-4. MALDI-TOF spectrum of Porph-DNA 2, found MW = 4231.58 Da, calculated MW = 4231.60 Da, for $[M+H]^+$.

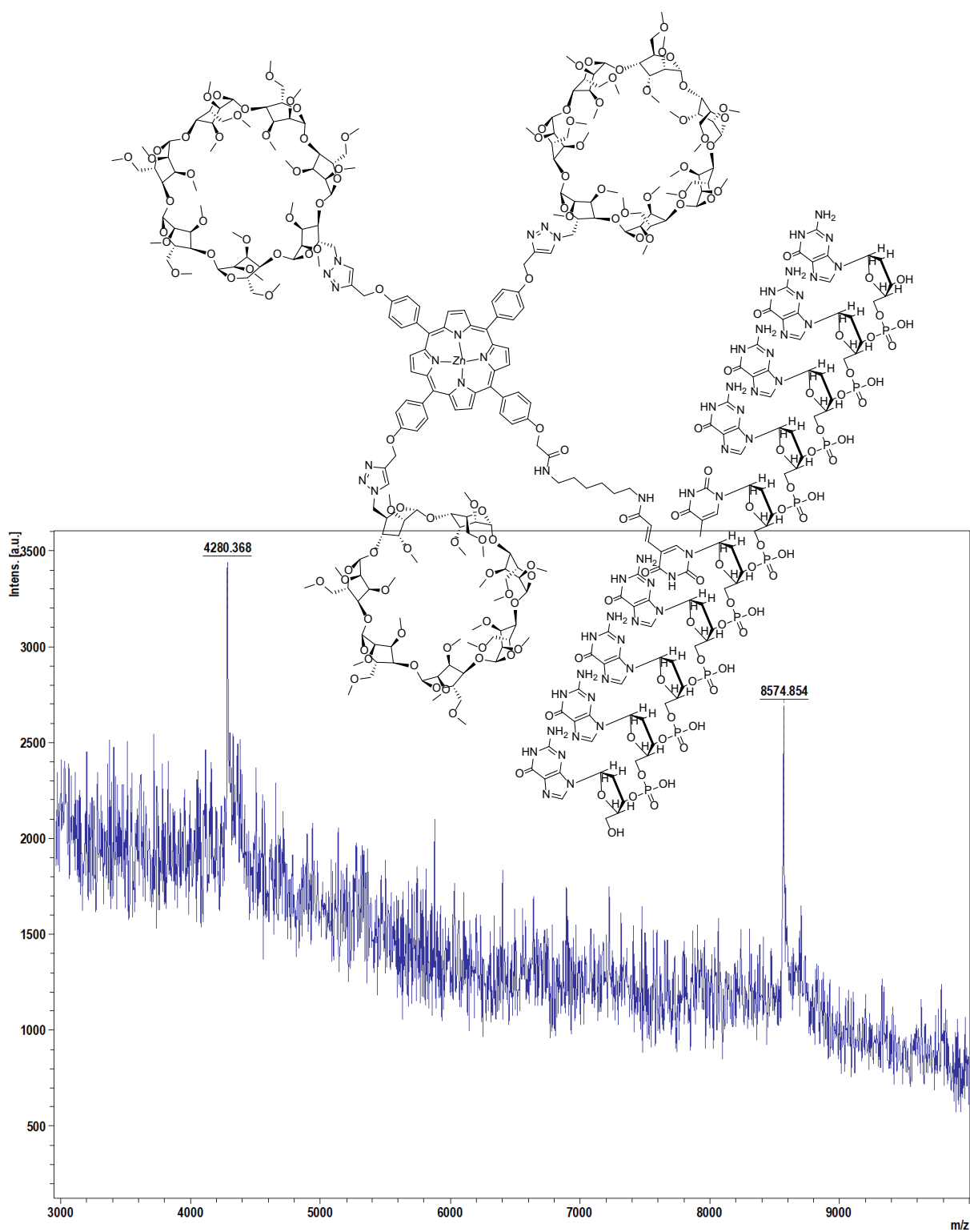


Figure S-5. MALDI-TOF spectrum of PL-DNA 2, found MW = 8574.85 Da, calculated MW = 8575.20 Da, for $[M+Na]^+$. Peak at 4280.37 represents $[M+2H]^{++}$.

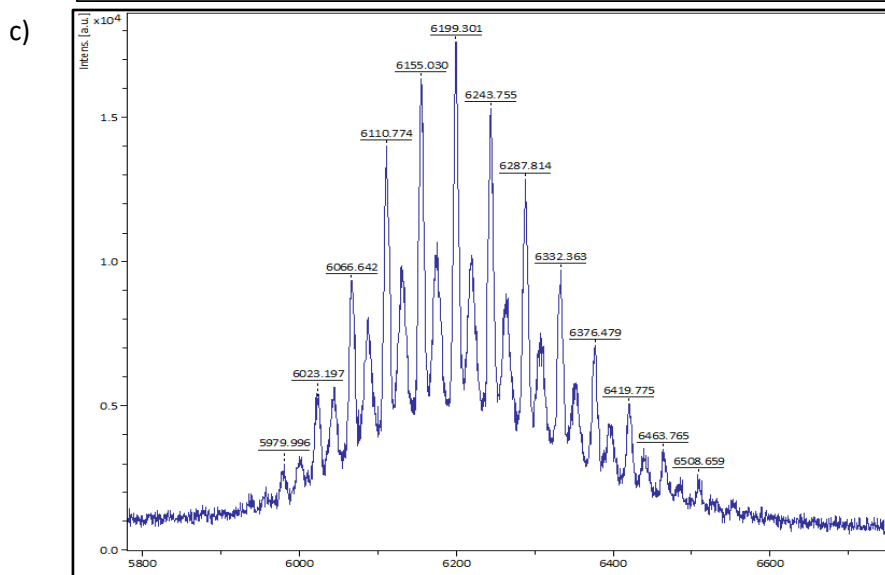
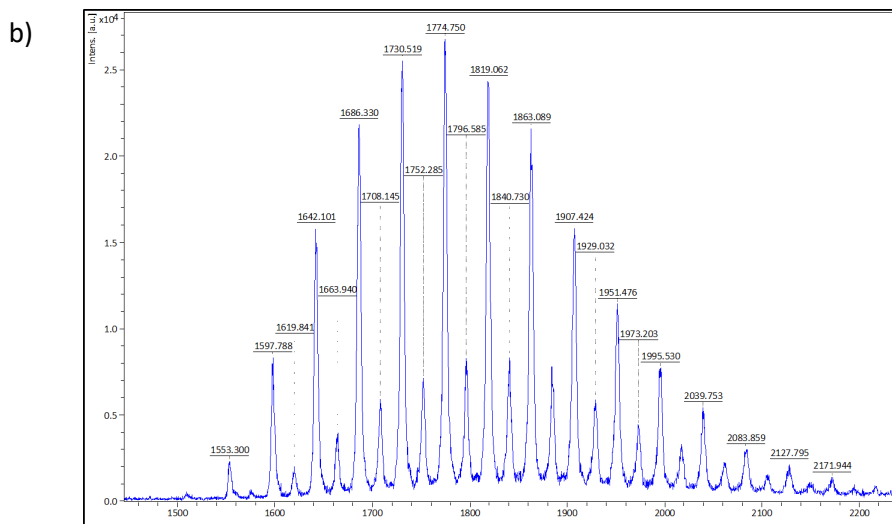
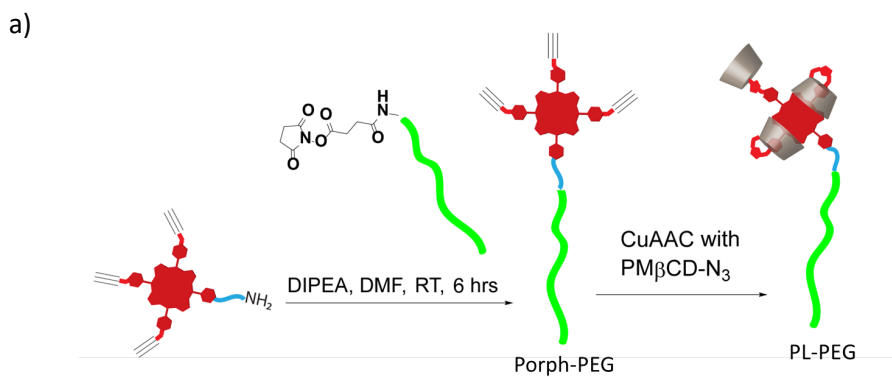


Figure S-6. a) Synthesis scheme of Porph-PEG and PL-PEG. b) MALDI-TOF analysis of Porph-PEG. Number Average MW observed, $M_n = 1830$ Da. c) MALDI-TOF analysis of PL-PEG. Number Average MW observed, $M_n = 6170$ Da.

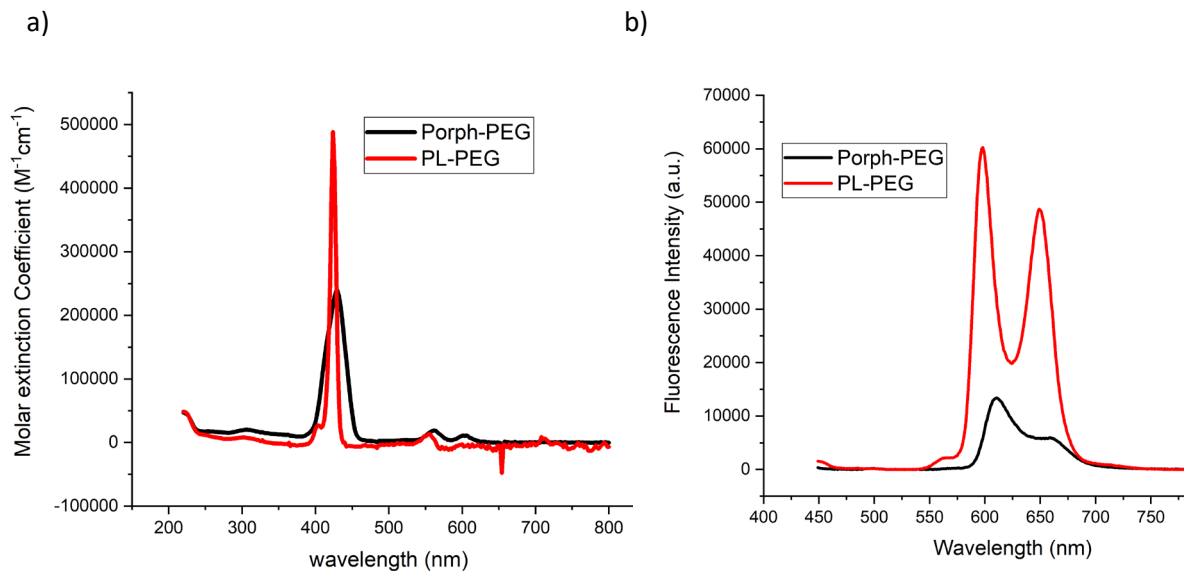


Figure S-7. a) UV-Vis absorption profiles of 1.5 μM solutions of Porph-PEG and PL-PEG in ultrapure water. **b)** Emission profiles of 1.5 μM solutions of Porph-PEG and PL-PEG in ultrapure water. Fluorescence enhancement was 4.5-fold in PL-PEG. Excitation was absorbance matched at 429 nm.

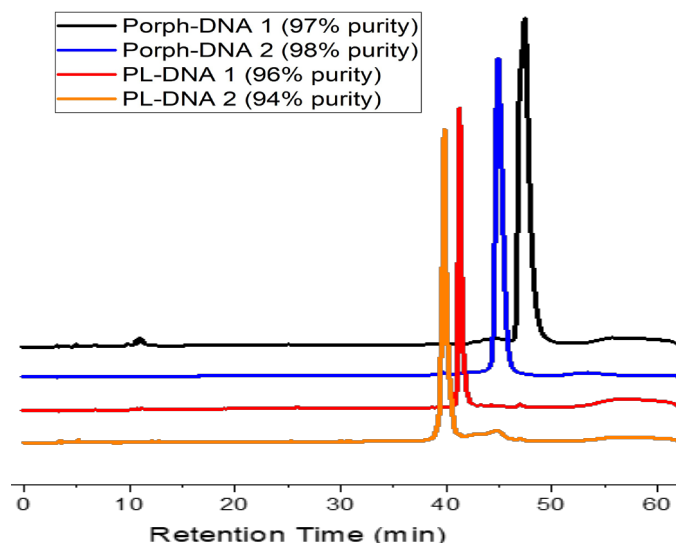


Figure S-8. RP-HPLC traces of porphyrin-DNA conjugates. The traces are obtained by running the already purified samples in an analytical (PLRP-S) HPLC column. The purity percentages were obtained by using the integrated peak areas of all the peaks in the HPLC trace. Further, these traces demonstrate the difference in hydrophilicity between the masked and unmasked porphyrin-DNA conjugates.

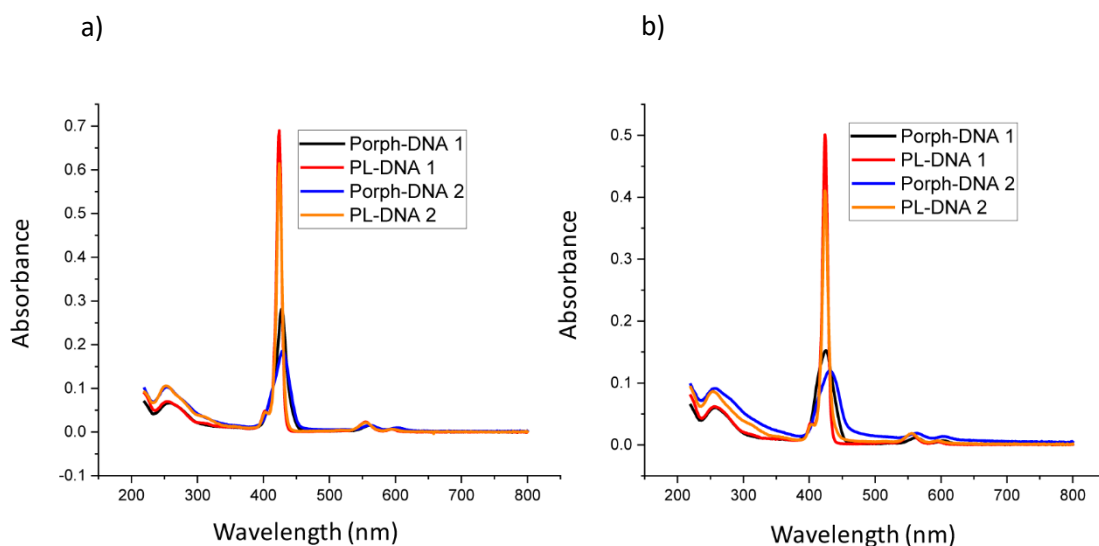


Figure S-9. a) UV-Vis absorption profiles of 1 μM porphyrin-DNA conjugates in pure water before annealing. b) UV-Vis absorption profiles of 1 μM porphyrin-DNA conjugates in buffers after annealing.

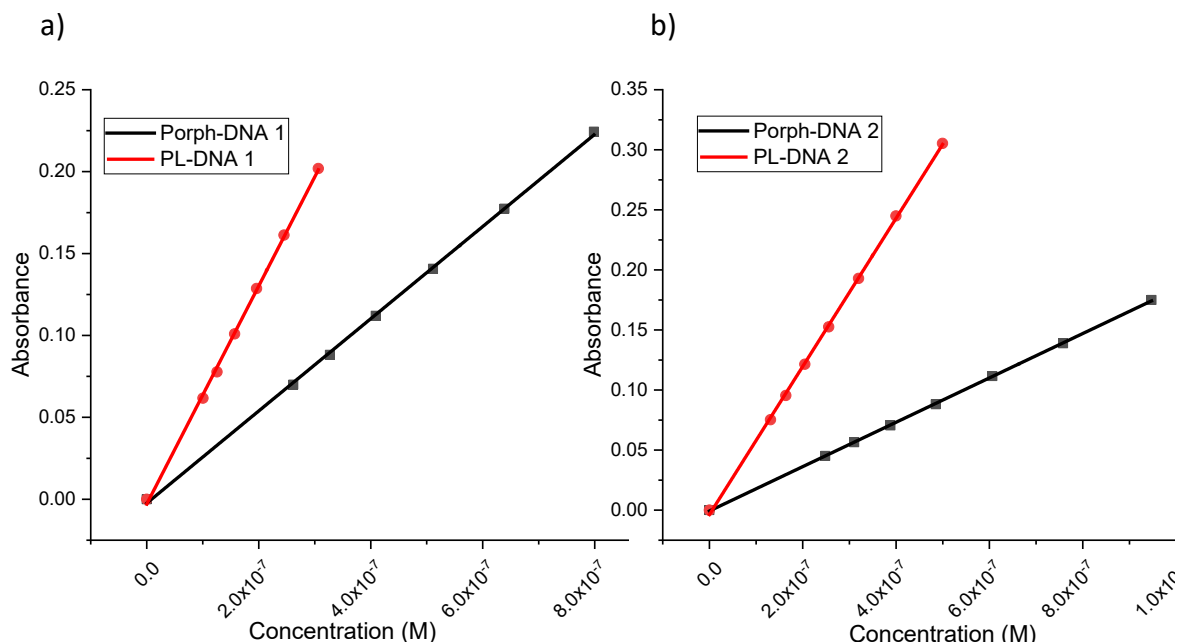


Figure S-10. a) Concentration vs absorbance calibration plots for Porph-DNA 1 and PL-DNA 1 solutions in water. $\epsilon = 281508 \text{ M}^{-1} \text{ cm}^{-1}$ at 428 nm for Porph-DNA 1 and $665710 \text{ M}^{-1} \text{ cm}^{-1}$ for PL-DNA 1 at 424 nm. **b)** Concentration vs absorbance calibration plots for Porph-DNA 2 and PL-DNA 2 solutions in water. $\epsilon = 184649 \text{ M}^{-1} \text{ cm}^{-1}$ for Porph-DNA 2 at 430 nm and $616621 \text{ M}^{-1} \text{ cm}^{-1}$ for PL-DNA 2 at 424 nm

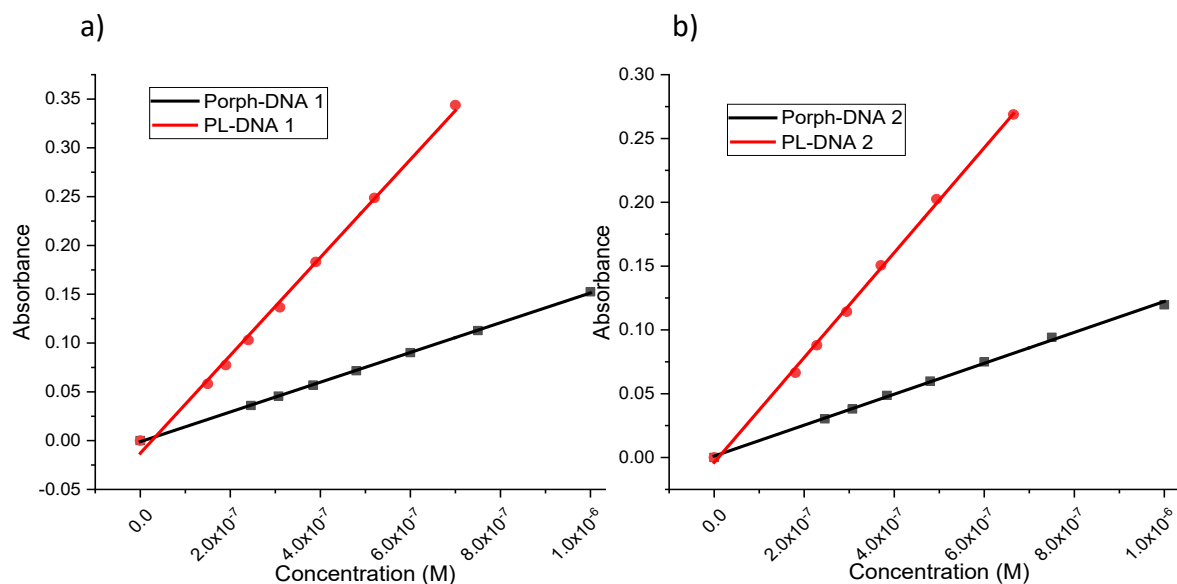


Figure S-11. a) Concentration vs absorbance calibration plots for Porph-DNA 1 and PL-DNA 1 solutions after annealing in 100 mM potassium phosphate buffer, pH 7.5. $\epsilon = 152428 \text{ M}^{-1} \text{ cm}^{-1}$ at 425 nm for Porph-DNA 1 and $501579 \text{ M}^{-1} \text{ cm}^{-1}$ for PL-DNA 1 at 424 nm. **b)** Concentration vs absorbance calibration plots for Porph-DNA 2 and PL-DNA 2 solutions after annealing in 50 mM Tris buffer with 50 mM KCl and 10 mM MgCl_2 , pH 7.5. $\epsilon = 121178 \text{ M}^{-1} \text{ cm}^{-1}$ for Porph-DNA 2 at 431 nm and $411079 \text{ M}^{-1} \text{ cm}^{-1}$ for PL-DNA 2 at 424 nm.

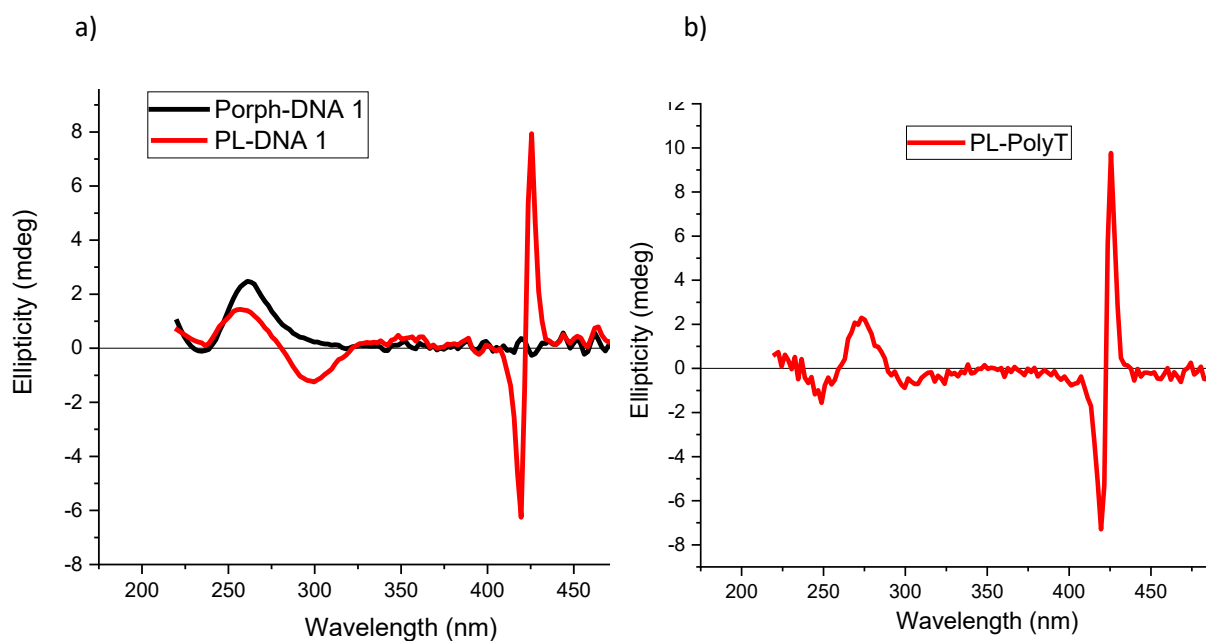


Figure S-12. a) CD spectra of Porph-DNA 1 and PL-DNA 1 in pure water before annealing as the representative profiles before induced assembly. b) CD spectra of PL-PolyT under annealing conditions in 100 mM potassium phosphate buffer, pH 7.5. Single Strand concentration of ODNs was 30 μ M.

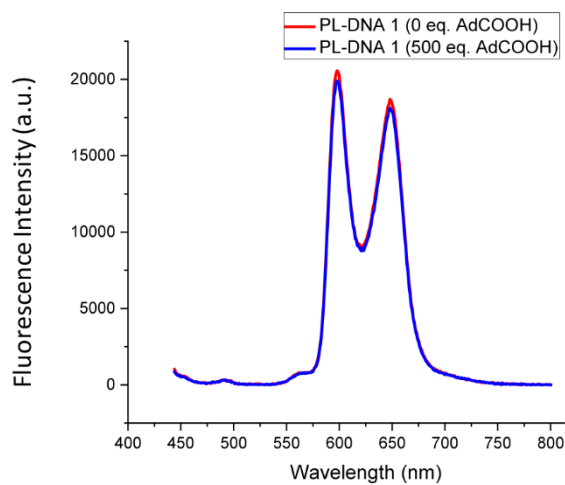


Figure S-13. Emission profiles of 0.4 μ M annealed solution of PL-DNA 1 with (500 eq) and without AdCOOH. Excitation was at 424 nm.

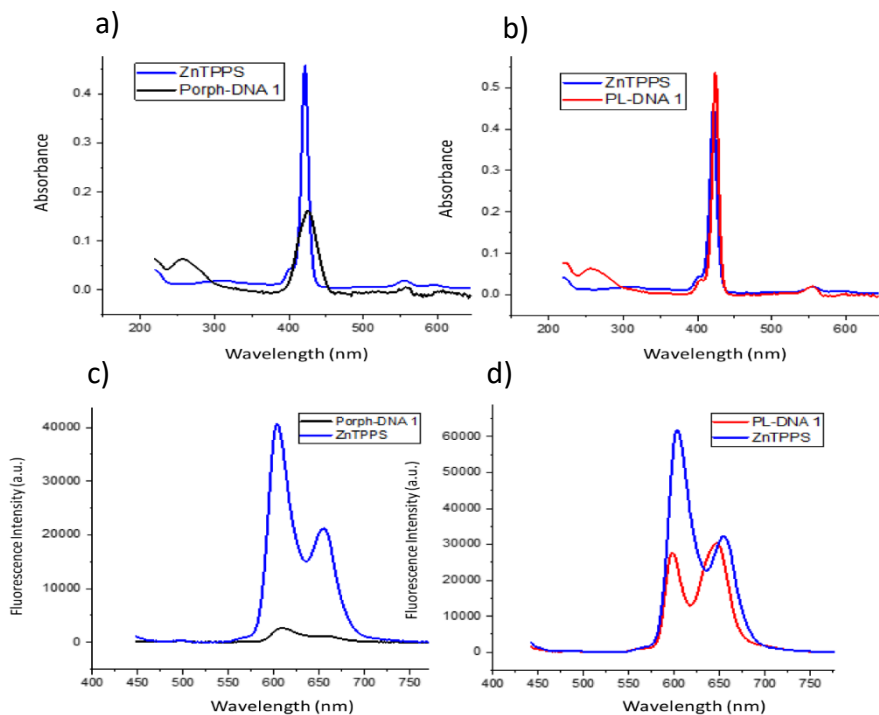


Figure S-14. Absorption and emission profiles of Porph-DNA 1 and PL-DNA 1 with ZnTPPS taken for the determination of quantum yield. Porphyrin-DNA conjugates were annealed and diluted to the concentration of 1 μM in the annealing buffer before taking the spectra **a)** UV-Vis absorption profiles of ZnTPPS and Porph-DNA 1. **b)** UV-Vis absorption profiles of ZnTPPS and PL-DNA 1. **c)** Emission profiles of ZnTPPS and Porph-DNA 1 excited at 428 nm (absorbance matched). **d)** Emission profiles of ZnTPPS and PL-DNA 1 excited at 422 nm (absorbance matched).

Fluorescence quantum yield was determined for the annealed samples of Porph/PL-DNA 1 and Porph/PL-DNA 2 using the standard reference zinc tetraphenylporphyrin tetrasulfonate (ZnTPPS). The reported fluorescence quantum yield value for ZnTPPS is 0.043.¹ All sample solutions were diluted to the concentration of 1 μM . The excitation wavelength was chosen by tallying the closely matching absorption values in the Soret region of the porphyrin core in the UV-Vis absorption profiles. The corresponding integrated emissions were calculated from the emission profiles. The following equation was used for the relative fluorescence quantum yield measurements.²

$$\phi_x = \phi_{st} \left(\frac{F_x}{F_{st}} \right) \left(\frac{f_{st}}{f_x} \right) \left(\frac{\eta_x^2}{\eta_{st}^2} \right)$$

Where,

ϕ_x and ϕ_{st} denote quantum yield for the unknown and the standard respectively. Similarly, F_x and F_{st} denote the integrated fluorescence intensity, f_x and f_{st} denote the absorption factor [$f = 1 - 10^{-A}$, where A is the absorbance values at the excitation wavelength], and η_x and η_{st} denote the refractive index of the solvent systems.

Results

ϕ_x for PL-DNA 1 = 0.027

ϕ_x Porph-DNA 1 = 0.003 (9-fold less)

Error = $\pm 10\%$

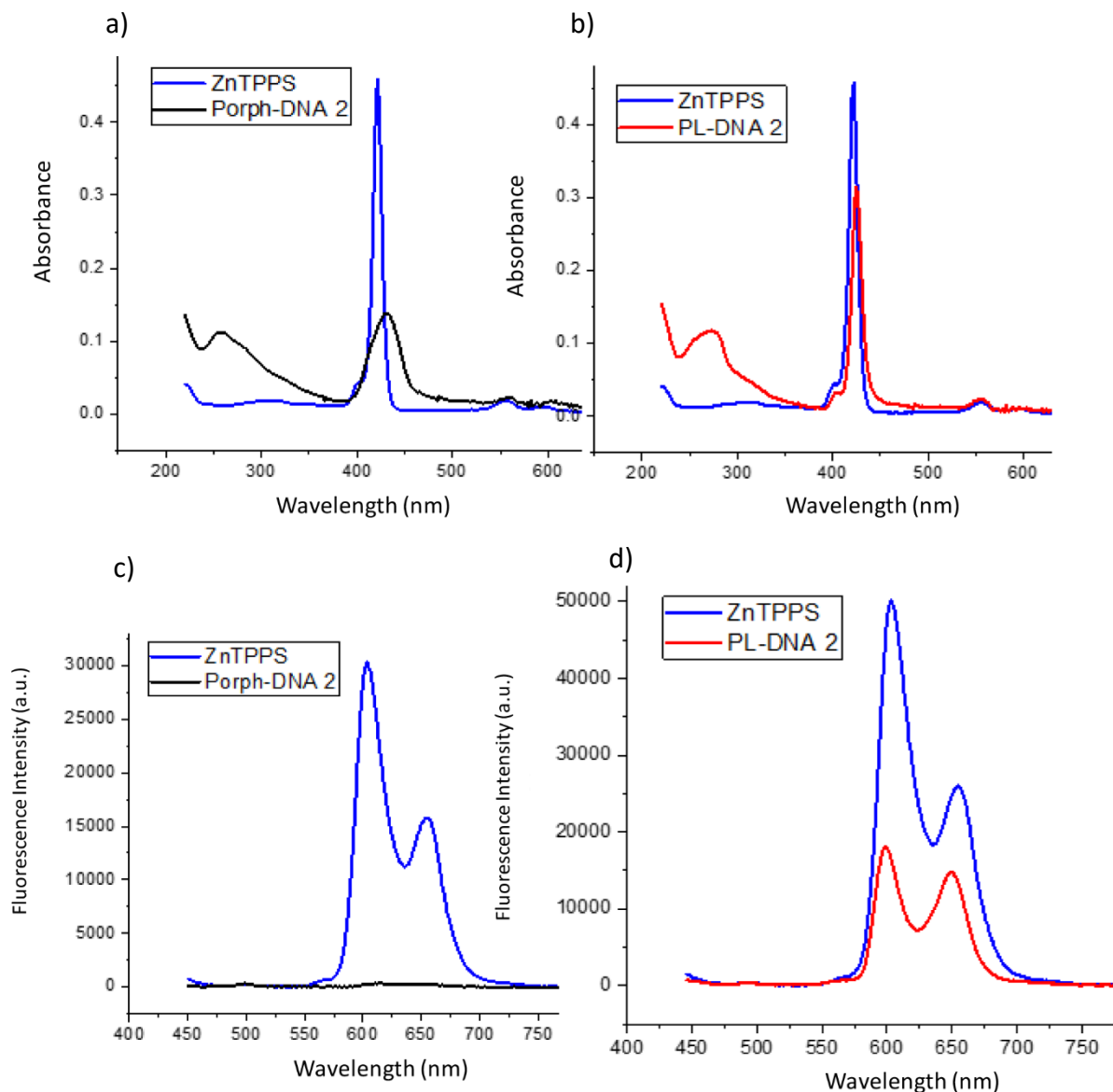


Figure S-15. Absorption and emission profiles of Porph-DNA 2 and PL-DNA 2 with ZnTPPS taken for the determination of quantum yield. Porphyrin-DNA conjugates were annealed and diluted to the concentration of 1 μM in the annealing buffer before taking the spectra. **a)** UV-Vis absorption profiles of ZnTPPS and Porph-DNA 2. **b)** UV-Vis absorption profiles of ZnTPPS and PL-DNA 2. **c)** Emission profiles of ZnTPPS and Porph-DNA 2 excited at 430 nm (absorbance matched). **d)** Emission profiles of ZnTPPS and PL-DNA 2 excited at 426 nm (absorbance matched).

Results

Φ_x for PL-DNA 2 = 0.0156

Φ_x Porph-DNA 2 = 0.0003 (**52-fold less**)

Error = \pm 10%

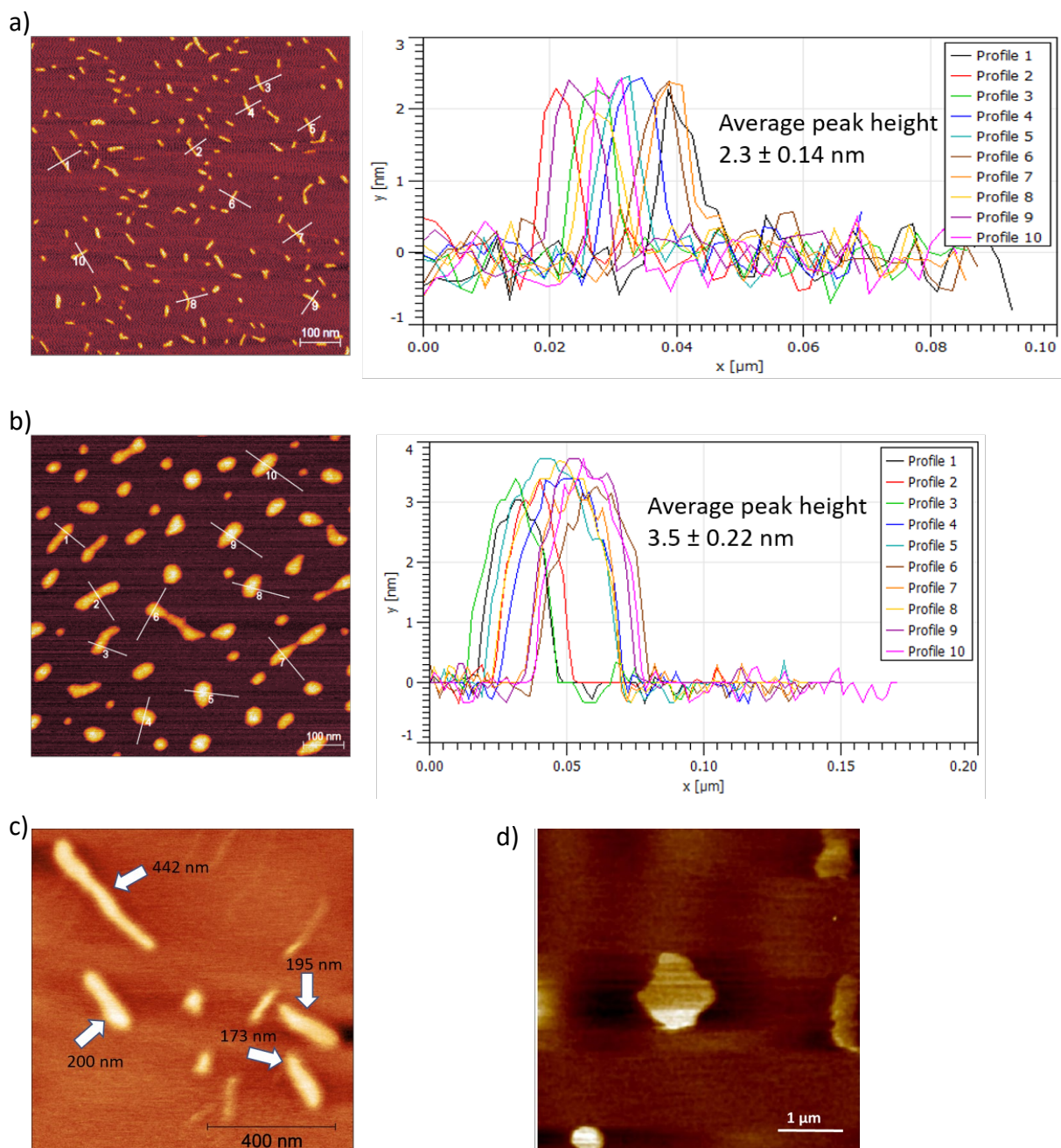


Figure S-16. a) AFM image of G-wires of parent DNA 2 (not conjugated with porphyrin). Average of the peak height is $2.3 \pm 0.14 \text{ nm}$ as seen in the height profiles. **b)** AFM image of annealed PL-DNA 2. Average of the peak height is $3.5 \pm 0.22 \text{ nm}$ as seen in the height profiles. Note: the smaller globular-looking species are ascribed to shorter G-wires because their AFM heights fall within the range of the longer wires. **c)** AFM image of annealed PL-DNA 2 featuring some longer wires observed. **d)** AFM image of annealed Porph-DNA 2.

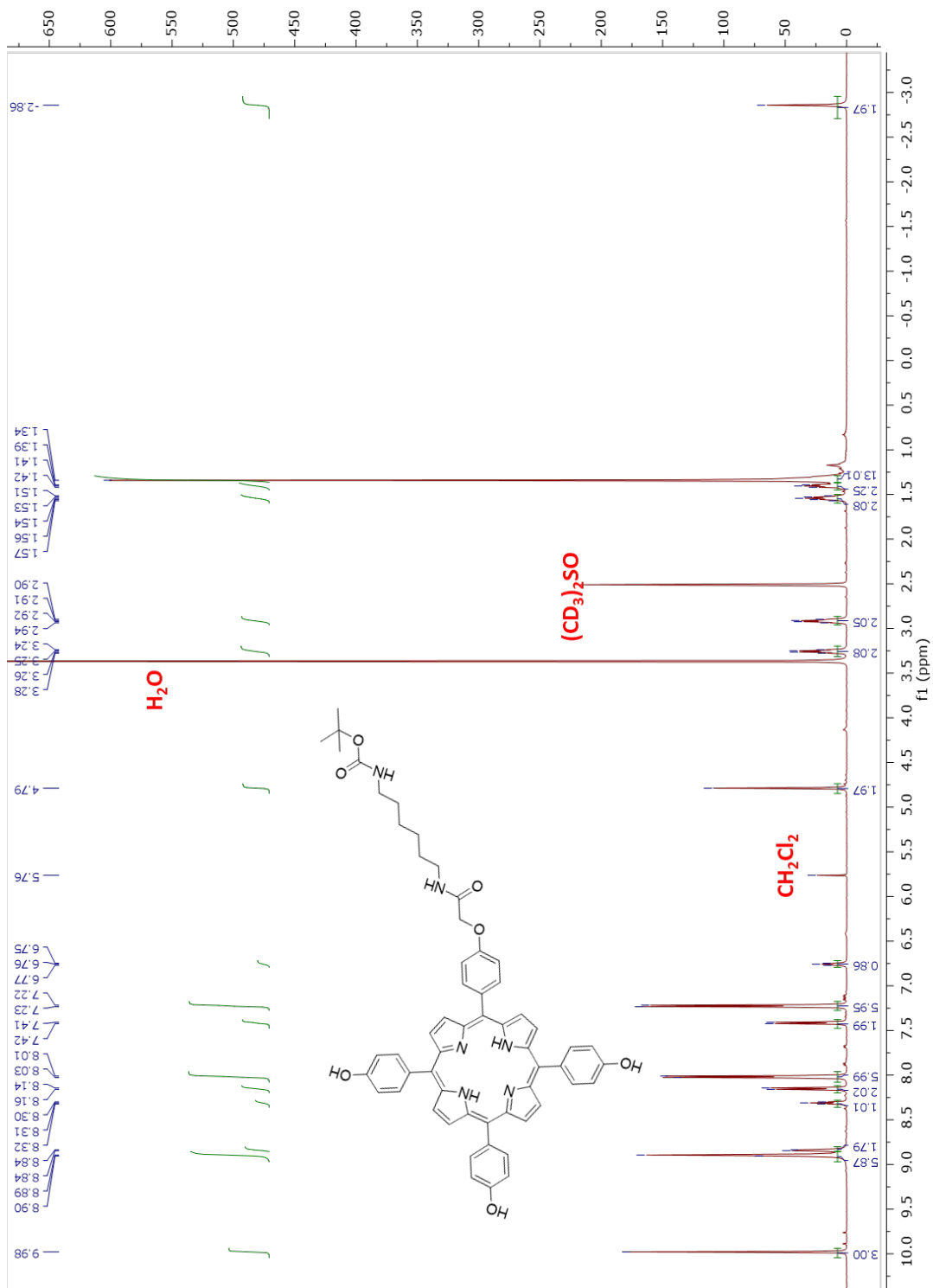


Figure S-17. ¹H NMR spectrum of compound 3

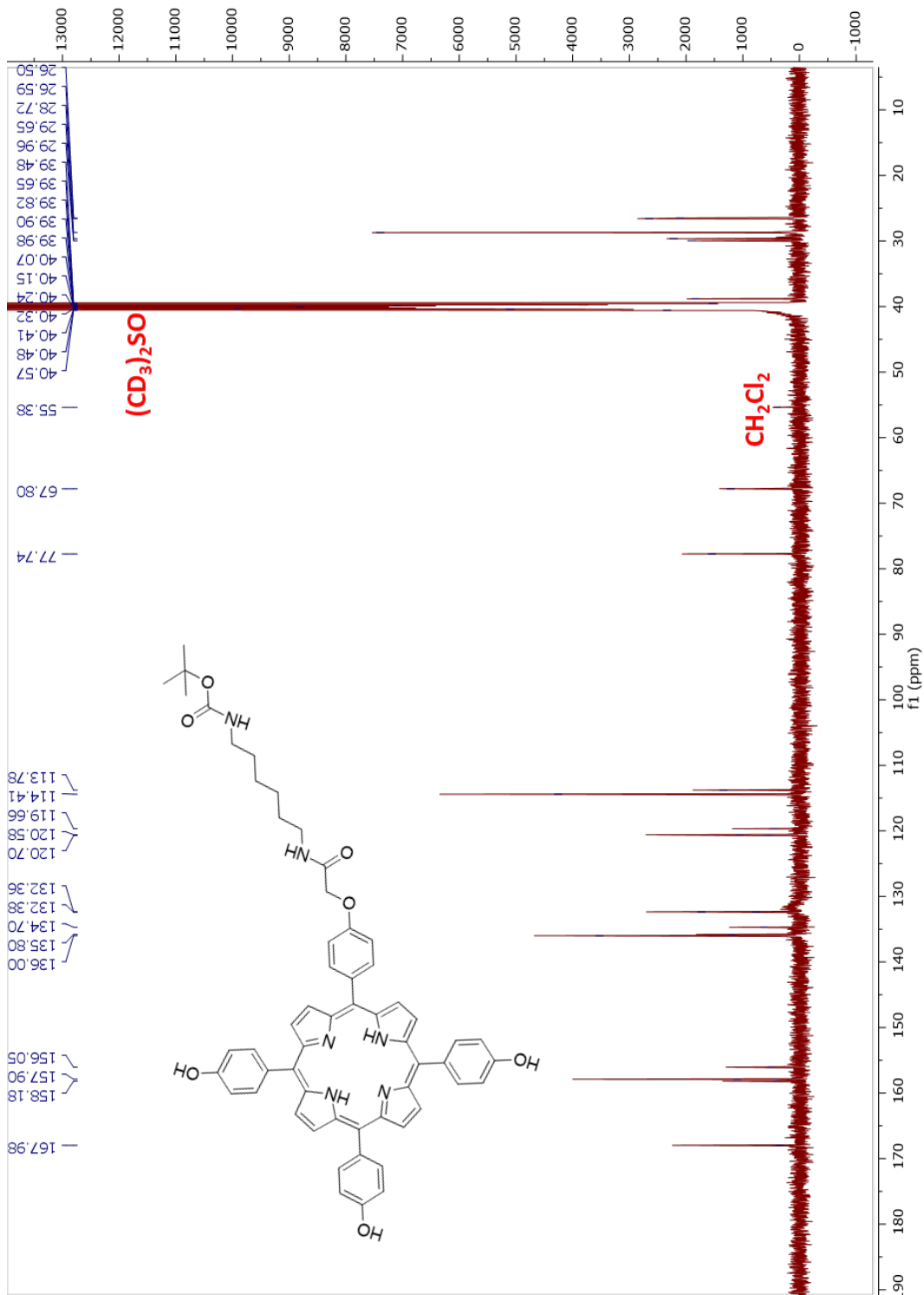


Figure S-18. CNMR spectrum of compound 3

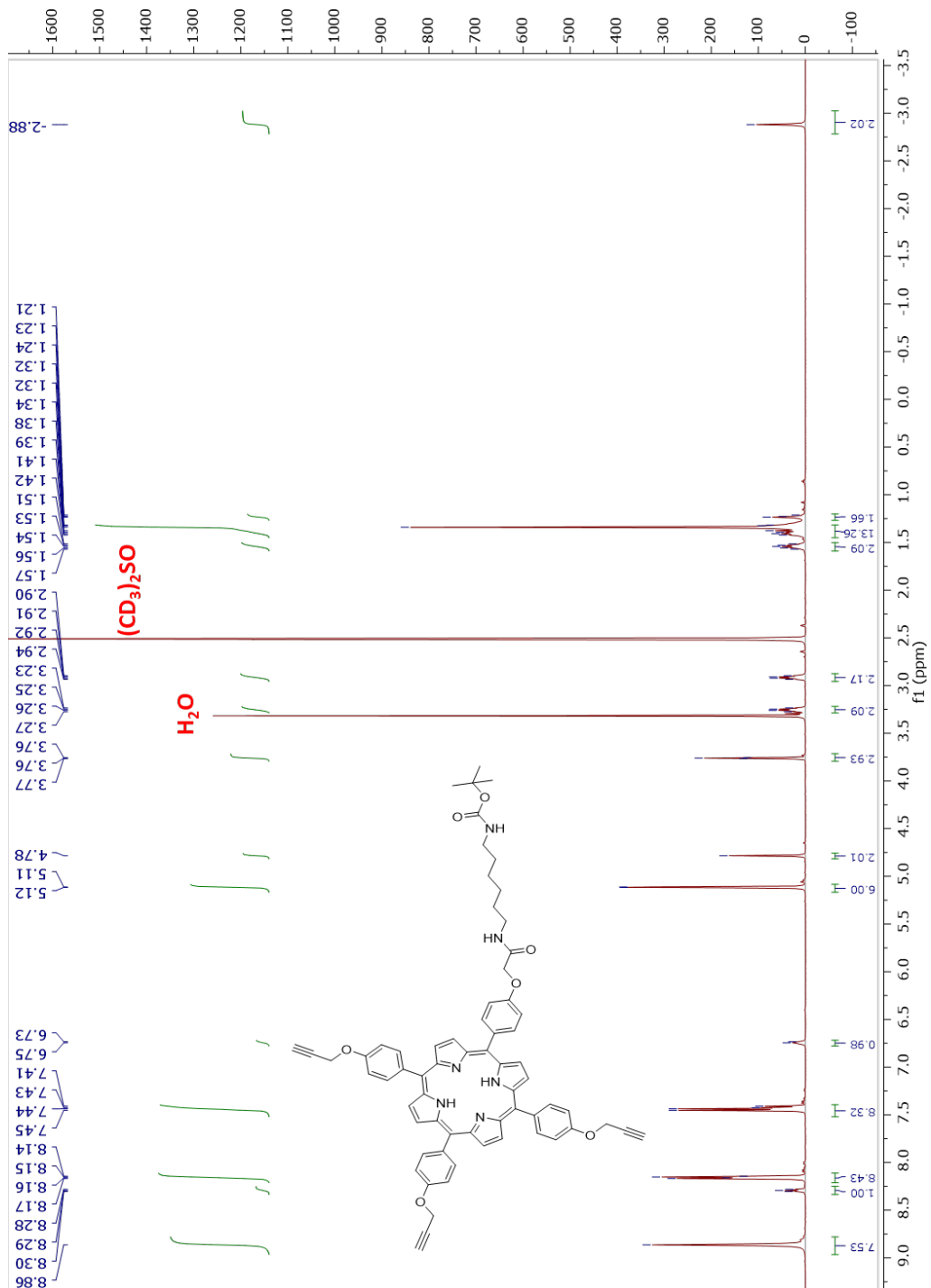


Figure S-19. HNMR spectrum of compound 4

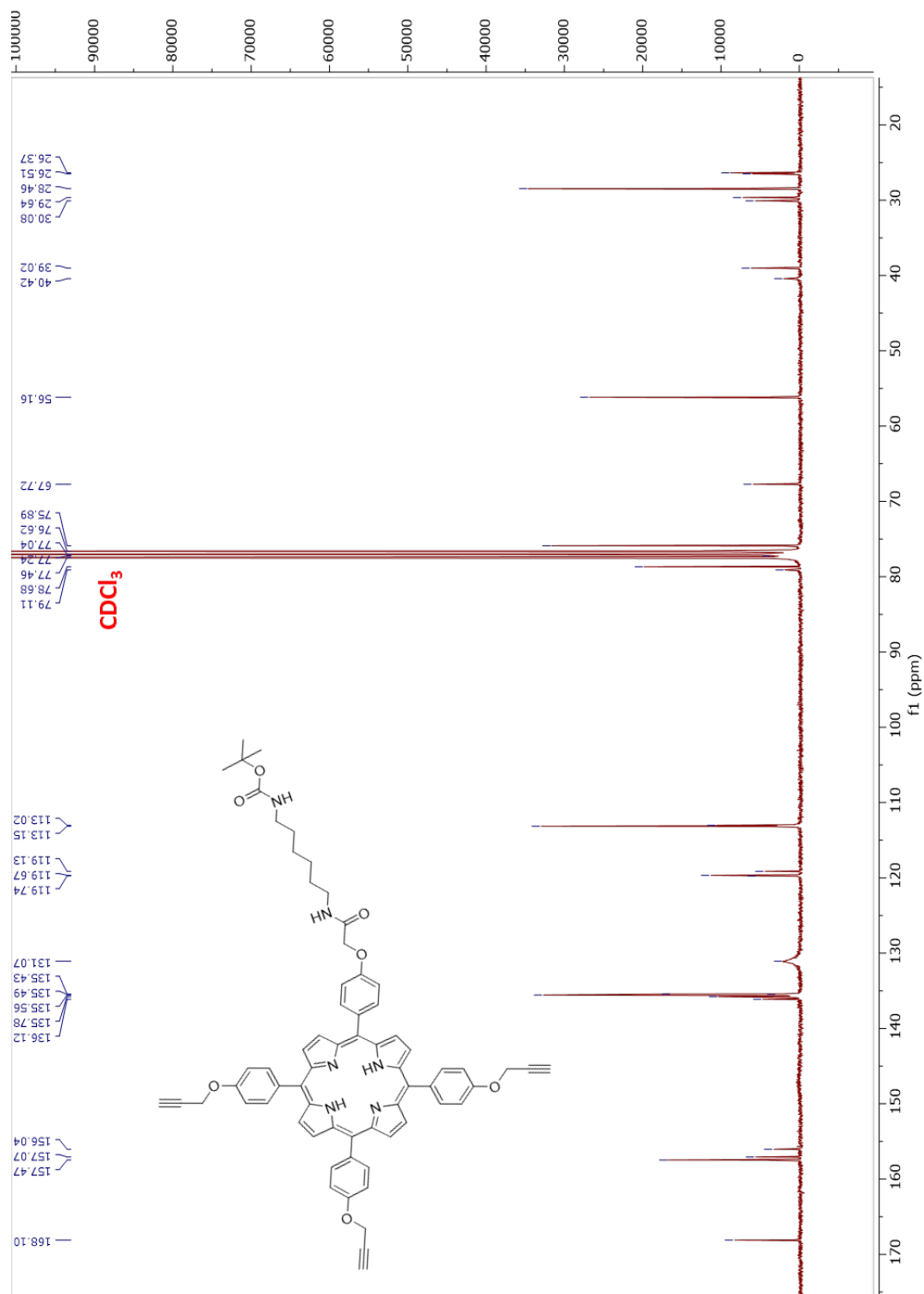


Figure S-20. CNMR spectrum of compound 4

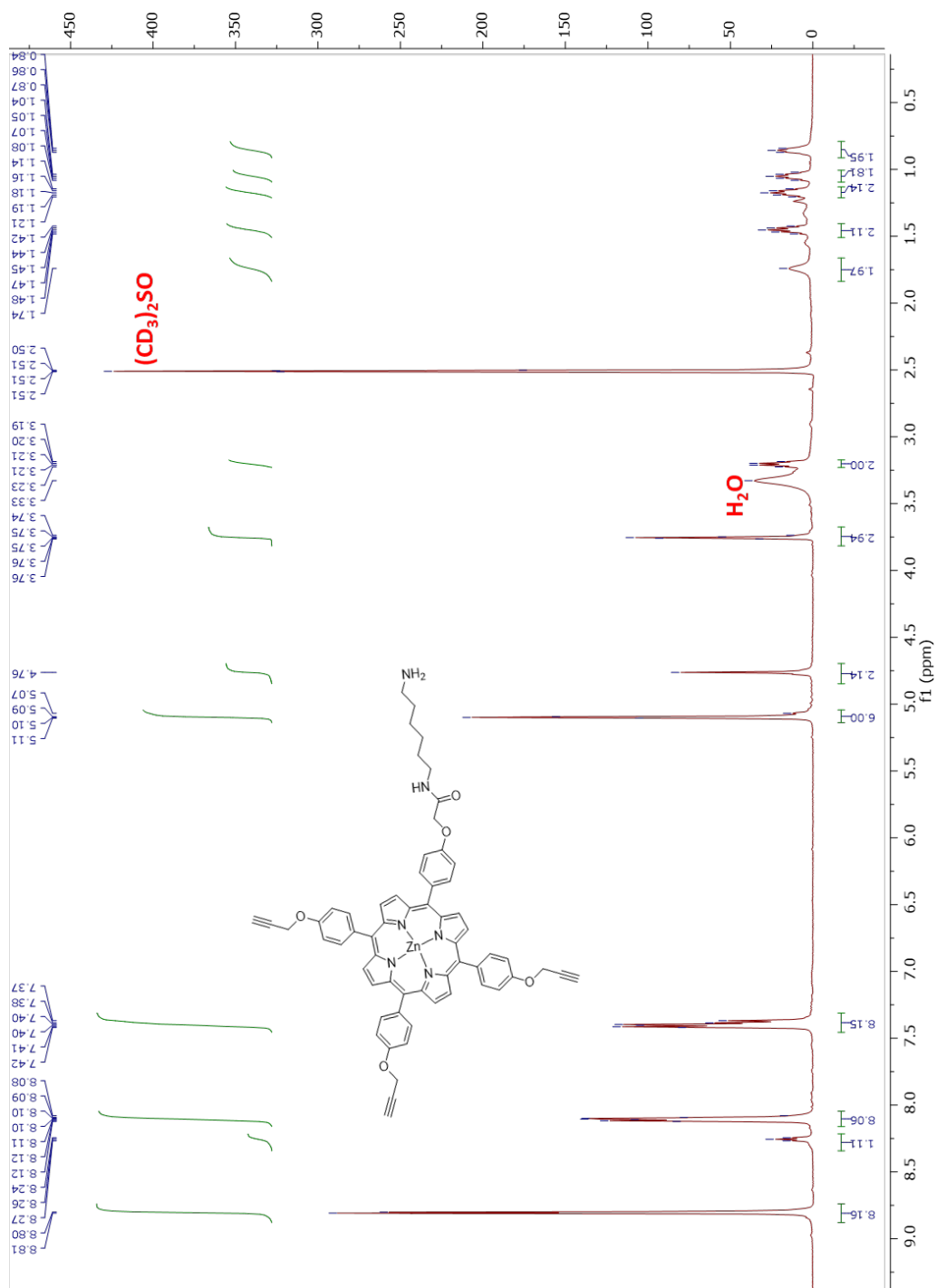


Figure S-21. ¹H NMR spectrum of Porphyrin 1

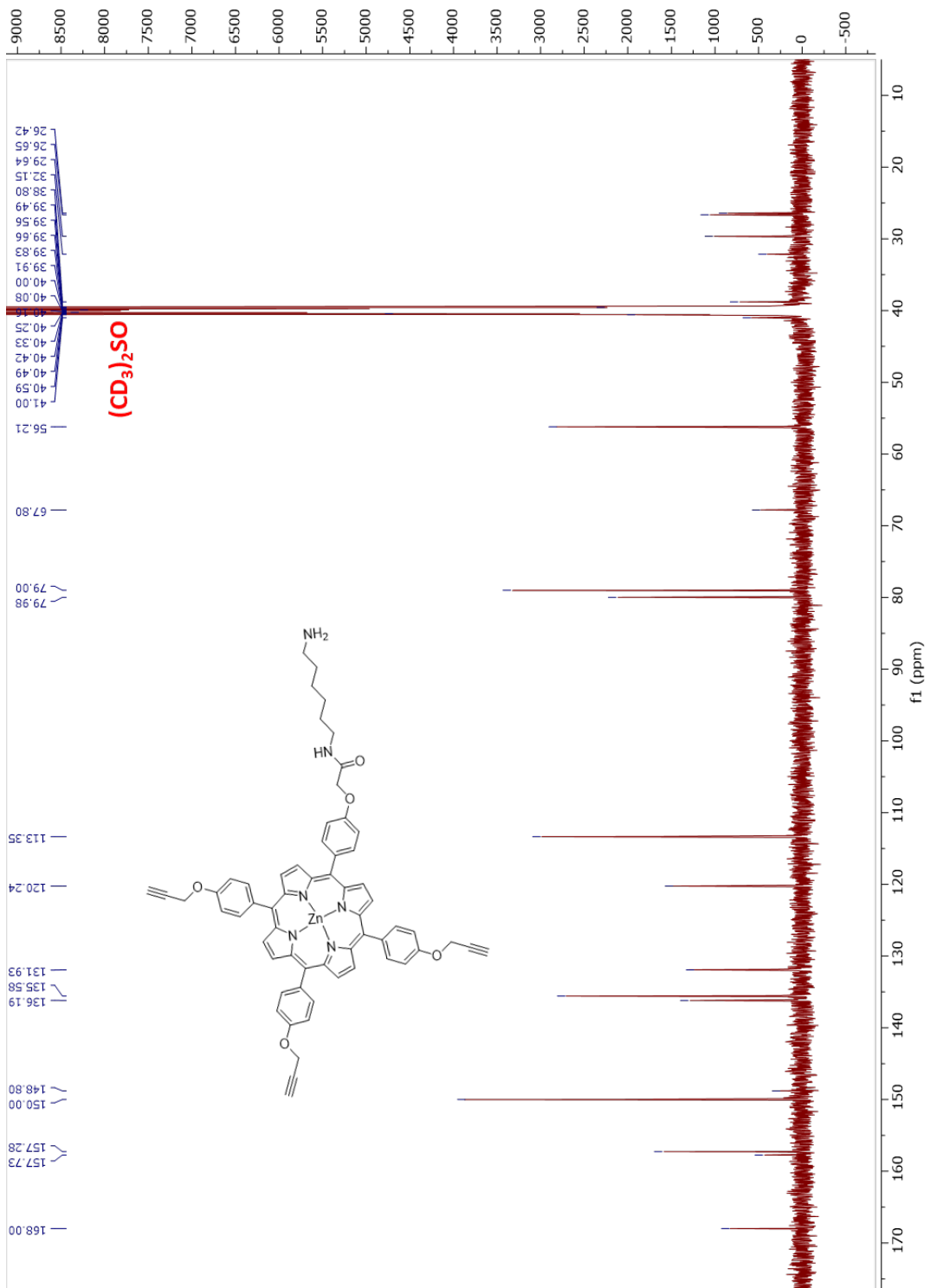


Figure S-22. CNMR spectrum of Porphyrin 1

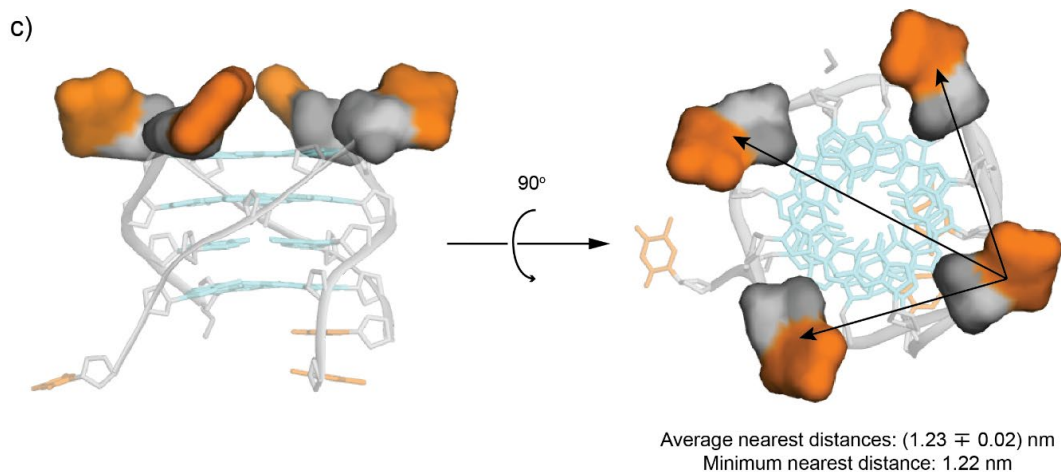
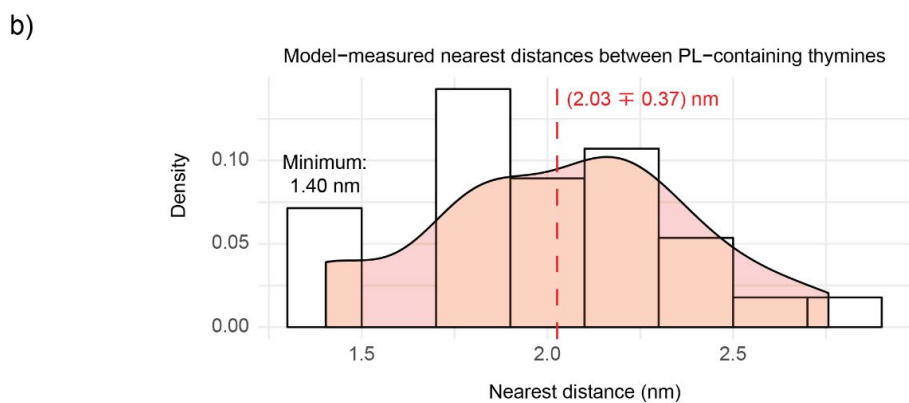
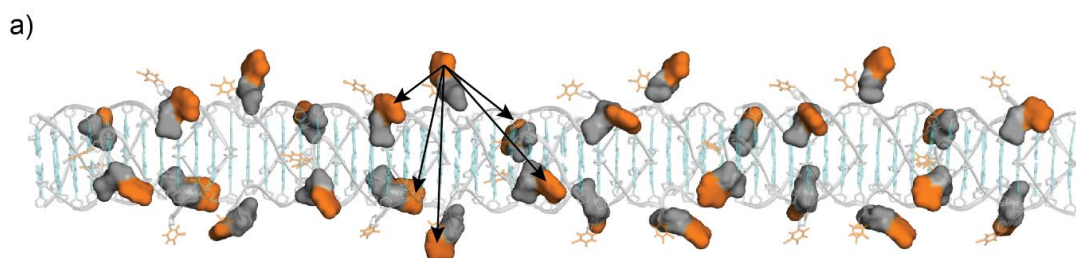


Figure S-23. a) Model of a G-wire generated from $G_4T_2G_4$ sequence ((2,2) Diagonal) was selected out of the three models shown by Phan et al.³ Highlighted in the surface representations are the thymidine residues that are attached to the PLs. Distances between methyl carbons of the neighboring PL-containing thymines are measured as shown with the arrows. **b)** Distribution histogram of the nearest measured distances from every PL-containing thymines (total amount of data is 28). The average nearest distance is 2.03 nm, and the minimum value is 1.40 nm. **c)** Side and top views of the structure of tetrameric G-quadruplex formed by TG_4T sequence (PDB code: 1S45).⁴ Highlighted in the surface representations are the thymidine residues that are attached to the PLs. Distances between O5' atoms of the PL-containing thymines are measured as shown with the arrows. Average nearest distance is 1.23 nm, and the minimum value is 1.22 nm.

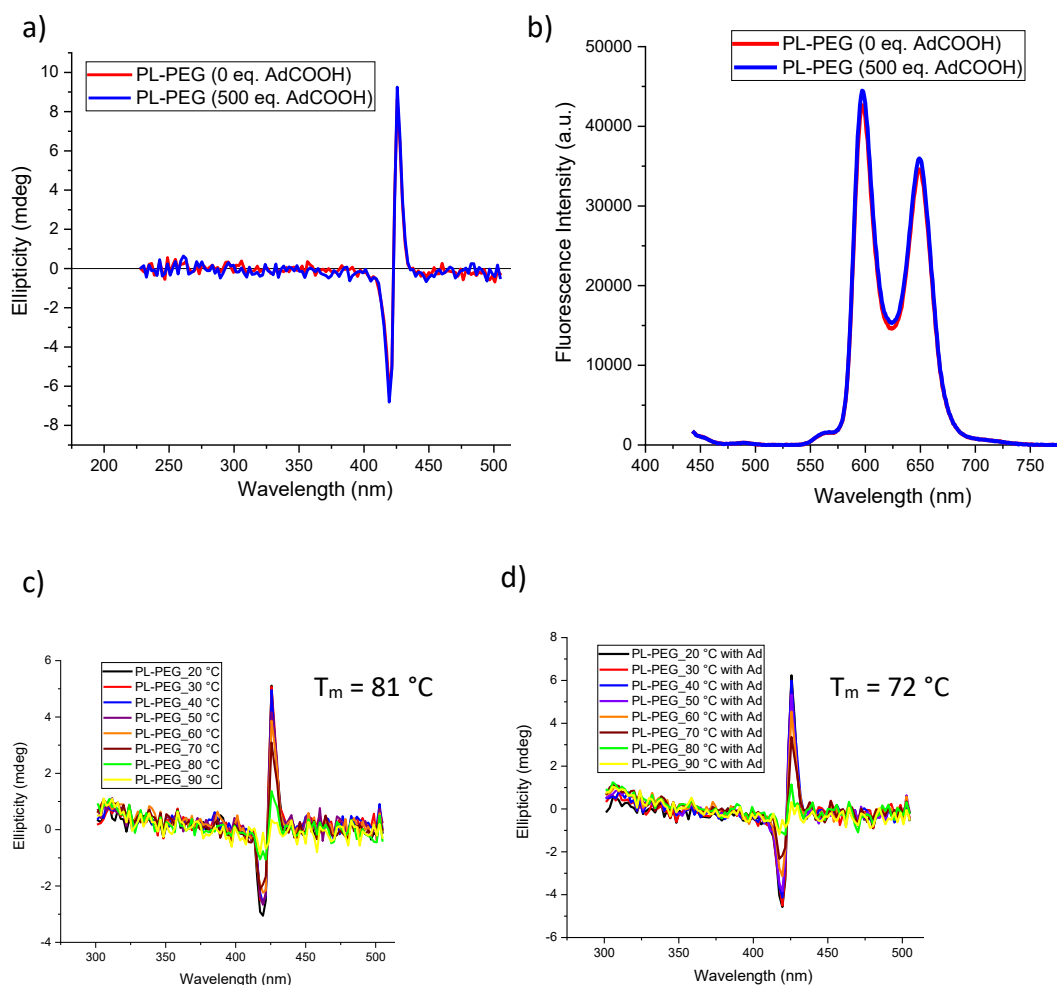


Figure S-24. a) CD spectra at room temp of 5 μM solutions of PL-PEG with (500 eq.) and without AdCOOH in 20 mM tris buffer, pH 7.5 (after 90 min incubation). **b)** Corresponding emission spectra at room temp of 1 μM solution of PL-PEG with (500 eq.) and without AdCOOH. Excitation was at 424 nm. **c)** Thermal denaturation CD spectra of a 5 μM solution of PL-PEG without AdCOOH. **d)** Thermal denaturation CD spectra of a 5 μM solution of PL-PEG with 500 eq. of AdCOOH. Note: spectra for panels c and d were taken after 72 hours of incubation. The melting temperatures (followed at 426 nm) is shown in the inset.

These studies illustrate that even 500 eq. of Ad-COOH does not displace the PL state (i.e., the intramolecular PM β CD-porphyrin complex) at room temperature. However, the PL state can be unraveled via thermal denaturation. In this case, the 500 eq. of Ad-COOH does have an effect in enhancing the thermally induced dis-assembly of the β CD caps from the porphyrin core.

DLS Experiments

All dynamic light scattering measurements were performed on a Nicomp ZLS Z3000 particle size analyzer (Particle Sizing Systems – Port Richey, FL), with a 50 mW laser diode (660 nm wavelength) and an avalanche photodiode (APD) detector. Measurements of scattered light were made at 90°, with data collected at 20 °C and processed using a non-negative least squares Nicomp analysis. Samples were filtered through 0.5-micron filter prior to DLS experiments. The single strand concentration of samples was 20 μ M.

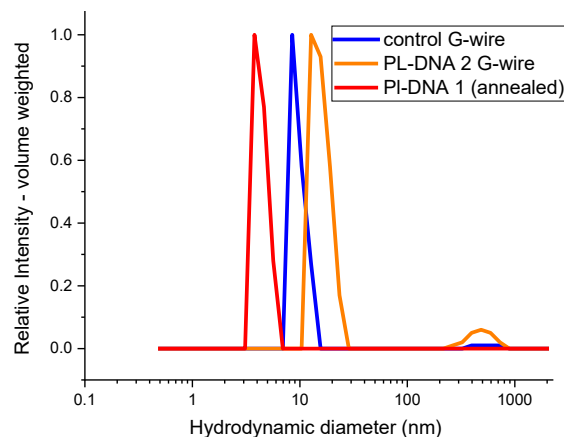


Figure S-25. Plots of hydrodynamic diameter (D_H) Vs relative intensity showing the volume distribution of particle sizes. **Results:** a) **PL-DNA 1 (annealed)** - $4.4 \text{ nm} \pm 0.6 \text{ nm}$. b) **control G-wire** of DNA 2- Peak 1 : $9.7 \text{ nm} \pm 1.5 \text{ nm}$ (98.6% volume), Peak 2: $522.9 \text{ nm} \pm 131.6$ (1.4% volume) c) **PL-DNA 2 G-wire** - Peak 1 : $15.3 \text{ nm} \pm 2.8 \text{ nm}$ (94.1% volume), Peak 2: $503.1 \text{ nm} \pm 127.1 \text{ nm}$ (5.9% volume). Note: the very large hydrodynamic diameter ($D_H > 500 \text{ nm}$) species that has low volume quantity is ascribed to aggregates formed by loose association of the G-wires. Such large size multipolyion systems are observed for polyelectrolyte solutions including DNA assemblies and G-wires.⁵

DLS Analysis

The dynamic light scattering (DLS) experiments provide the hydrodynamic diameter (D_H) of a sphere that has the same diffusion coefficient (D) as the particle being investigated. For the annealed PL-DNA 1 case, the tetramolecular quadruplex can be assumed to be spherical and hence the obtained diameter ($4.4 \text{ nm} \pm 0.6 \text{ nm}$) likely represents the G-quadruplex of PL-DNA 1. For annealed samples of PL-DNA 2 a significantly larger D_H value ($15.3 \text{ nm} \pm 2.8 \text{ nm}$) was obtained suggesting the presence of G-wires. In order to estimate the average length of the G-wires we used the theory proposed by Tirado and Garcia de la Torre for circular cylinders (rods) of finite length.^{6,7} Specifically, using equations 1 and 2 (*infra*), we determined what range in the length value (L) given a fixed diameter for PL-DNA 2 G-wire of 3.5 nm (obtained from AFM) provides a theoretical D that corresponds to the experimental D (determined from converting the DLS obtained D_H to D via the Stoke-Einstein relationship).

$$D = \frac{K_B T}{3\pi\eta L} (\ln p + v) \dots\dots\dots 1$$

Where, D is translational diffusion coefficient, K_B is Boltzmann constant, T is absolute temperature, η is viscosity of the solvent, L is length of the rods, and p is ratio of the length (L) of rods to the diameter (d) of the rods (i.e., $p = L/d$). The last term v is the end-effect correction term given by equation 2.

$$v = 0.312 + 0.565/p - 0.100/p^2 \dots\dots\dots 2$$

From this analysis, the average lengths of the PL-DNA 2 G-wires (in solution) was estimated to be in the range between 40 - 45 nm. Further, the average lengths of control DNA 2 G-wires is in the range of 25 - 30 nm (when a rod diameter of 2.3 nm is used).

It is also important to mention that for the non-annealed sequences no significant light scattering signals were detected on the DLS. This is not surprising since these samples are not self-assembled and our working concentrations are low (20 μ M).

REFERENCES

- (1) Kalyanasundaram, K.; Neumann-Spallart, M. Photophysical and Redox Properties of Water-Soluble Porphyrins in Aqueous Media. *J. Phys. Chem.* **1982**, *86*, 5163–5169.
- (2) Würth, C.; Grabolle, M.; Pauli, J.; Spieles, M.; Resch-Genger, U. Relative and Absolute Determination of Fluorescence Quantum Yields of Transparent Samples. *Nat. Protoc.* **2013**, *8*, 1535–1550.
- (3) Bose, K.; Lech, C. J.; Heddi, B.; Phan, A. T. High-Resolution AFM Structure of DNA G-Wires in Aqueous Solution. *Nat. Commun.* **2018**, *9*, 1959.
- (4) Cáceres, C.; Gouyette, C.; Parkinson, G.; Wright, G.; Subirana, J. A. A Thymine Tetrad in d(TGGGGT) Quadruplexes Stabilized with Tl⁺/Na⁺ Ions. *Nucleic Acids Res.* **2004**, *32*, 1097–1102.
- (5) Ilc, T.; Šket, P.; Plavec, J.; Webba da Silva, M.; Drevenšek-Olenik, I.; Spindler, L. Formation of G-Wires: The Role of G:C-Base Pairing and G-Quartet Stacking. *J. Phys. Chem. C* **2013**, *117*, 23208–23215.
- (6) Tirado, M. M.; Martínez, C. L.; de la Torre, J. G. Comparison of Theories for the Translational and Rotational Diffusion Coefficients of Rod-like Macromolecules. Application to Short DNA Fragments. *J. Chem. Phys.* **1984**, *81*, 2047–2052.
- (7) Spindler, L.; Rigler, M.; Drevenšek-Olenik, I.; Ma'ani Hessari, N.; Webba da Silva, M. Effect of Base Sequence on G-Wire Formation in Solution. *J. Nucleic Acids* **2010**, *2010*, 431651.